Electronic Supplementary Material (ESI) for Inorganic Chemistry Frontiers.

Supporting Information

Two isomorphous azide/formate Mn(II) coordination polymers show spin-canted antiferromagnetism only in the formate system

Jiao-Yang Wang[a], Qian Yang[b]*, Yi-Quan Zhang[c]*, Guang-Bo Che[d], Jiong-Peng Zhao[a]* and Fu-Chen Liu[a,d]*

[a] School of Chemistry and Chemical Engineering, TKL of Organic Solar Cells and Photochemical Conversion, Tianjin University of Technology, Tianjin, China 300384

[b] School of Science, Tianjin University of Science&Technology

[c] Jiangsu Key Laboratory for NSLSCS, School of Physical Science and Technology, Nanjing Normal University, Nanjing 210023, P. R. China

[d] Key Laboratory of Preparation of Environmental Friendly, Jilin Normal University, Ministry of Education, Changchun, 130103,China

E-mail: horryzhao@yahoo.com, qyang1984@tust.edu.cn, zhangyiquan@njnu.edu.cn and fuchenliutj@yahoo.com

Materials and Physical Measurements.

All the chemicals used for synthesis are of analytical grade and commercially available. pyrazine-2-carboxylic acid and methanol were purchased from commercial sources and used as received. The solid product was separated by filtration.

Elemental analyses (C, H, N) were performed on a Perkin-Elmer 240C elemental analyzer. The X-ray powder diffraction (XRPD) was recorded on a Rigaku D/Max-2500 diffractometer at 50 kV, 40 mA for a Cu-target tube, and a graphite monochromator. Simulation of the XRPD spectra was carried out by the single-crystal data and diffraction-crystal module of the Mercury (Hg) program available free of charge via the Internet at http://www.iucr.org.

Magnetic data were collected using crushed crystals of the sample on a Quantum Design MPMS-XL SQUID magnetometer equipped with a 5 T magnet. The data were corrected using Pascal's constants to calculate the diamagnetic susceptibility, and an experimental correction for the sample holder was applied.

X-Ray Data Collection and Structure Determinations.

X-ray single-crystal diffraction data for complexes **1-2** were collected on a Bruker Smart 1000 CCD diffractometer at 293(2) K with MoK α radiation (λ=0.71073 Å) in the ω scan mode. The program SAINT[S1] was used for integration of the diffraction profiles. All of the structures were solved using direct methods using the SHELXS program of the SHELXTL package and refined using fullmatrix least-squares methods with SHELXL (semiempirical absorption corrections were applied using the SADABS program).[S2] Metal atoms in each complex were located from the *E*-maps, and other non-hydrogen atoms were located in successive difference Fourier syntheses and refined with anisotropic thermal parameters on F^2.The hydrogen atoms of the ligands were generated theoretically onto the specific atoms and refined isotropically with fixed thermal factors. Detailed crystallographic data are summarized in Table S1.

Synthesis of complexes 1 and 2.

$[Mn(\mathbf{L})(N_3)\cdot MeOH]_n$. (**1**)

A mixture of **1** mmol $MnCl_2.4H_2O$(1mmol), H**L** (H**L** = pyrazine-2-carboxylic acid) (0.5mmol) and NaN_3(3mmol) in methanol solution (10ml) was sealed in a teflon-lined stainless steel vessel, heated at 140 ℃ for 2 days under autogenous pressure, and then cooled to room temperature. Yellow cube crystals of **1** were harvested in about 20% yield (based on H**L**).

$[Mn(\mathbf{L})(HCO_2)\cdot MeOH]_n$. (**2**)

A mixture of $Mn(HCO_2)_2\cdot 4H_2O$ (1.5 mmol), H**L** (H**L** = pyrazine- 2-carboxylic acid) (0.75mmol) in methanol solution (10ml) was sealed in a teflon-lined stainless steel vessel, heated at 140 ℃ for 2 days under autogenous pressure, and then cooled to room temperature. Yellow cube crystals of **2** were harvested in about 20% yield (based on H**L**).

Table S1 Crystal Date and Structure Refinements for **1** and **2**.

	1	**2**
Chemical formula	$C_6H_7MnN_5O_3$	$C_7H_7MnN_2O_5$
Formula weight	252.11	254.08
Crystal system	Orthorhombic	Orthorhombic
space group	$P2_12_12_1$	$P2_12_12_1$
a (Å)	8.7052(17)	9.2234 (18)
b (Å)	10.349(2)	9.795 (2)
c (Å)	10.742(2)	10.601 (2)
V (Å³)	967.8(3)	957.7 (3)
Z	4	4
GOF	1.154	1.155
D/g cm⁻³	1.730	1.762
μ (mm⁻¹)	1.359	1.381
Flack	0.14(6)	0.07(5)
Crystal size (mm)	0.2 × 0.15 × 0.2	0.20 × 0.15 × 0.14
T/K	293(2)	293(2)
ΛMoK\a (Å)	0.71073	0.71073
R^a/R^b	0.072/0.168	0.101/0.233

$^aR = \Sigma||F_o| - |F_c||/\Sigma|F_o|$. $^bR_w = [\Sigma[w(F_o^2 - F_c^2)^2]/\Sigma w(Fo^2)^2]^{1/2}$.

Table S2. Selected Bond Lengths [A°] and Angles for Complexes **1** and **2** [deg]

1

Mn(1)-O(2)#1	2.131(5)	Mn(1)-O(1)	2.196(5)
Mn(1)-N(1)	2.177(7)	Mn(1)-N(4)#2	2.336(5)
Mn(1)-N(3)#3	2.177(7)	Mn(1)-N(5)	2.344(5)

O(2)#1-Mn(1)-N(1)	89.7 (3)	N(3)#2-Mn(1)-N(4)#3	90.8(3)
O(2)#1-Mn(1)-N5	111.9(2)	O(1)-Mn(1)-N(4)#2	89.14(19)
N(1)-Mn(1)-N(3)#2	94.8(3)	N(3)#2-Mn(1)-O2#1	89.8(2)
O(2)#1-Mn(1)-O(1)	173.83(18)	N(1)-Mn(1)-N(5)	89.7(2)
N(1)-Mn(1)-O(1)	94.6(3)	N(3)#2-Mn(1)-N(5)	157.8(2)
N(3)#3-Mn(1)-O(1)	85.4(2)	O(1)-Mn(1)-N(5)	72.6(2)
O(2)#1-Mn(1)-N(4)#3	87.04(19)	N(4)#3-Mn(1)-N(5)	86.2(2)
N(1)-Mn(1)-N(4)#3	173.5(3)		

Summetry code: #1 3/2-x, 2-y, 1/2+z; #2 1-x, 1/2+y, 3/2-z; #3 -x, 1/2+y, 3/2-z.

2

Mn(1)-O(2)	2.137 (8)	Mn(1)-O(4)#2	2.155 (8)
Mn(1)-O(1)#3	2.122 (8)	Mn(1)-N(2)#1	2.337 (9)
Mn(1)-O(3)	2.203 (8)	Mn(1)-N(1)	2.315 (9)

O(1)#3-Mn1-O(3)	95.6 (3)	O(2)-Mn(1)-N(1)	152.9 (3)
O(2)-Mn(1)-O(3)	83.5 (3)	O(1)#3-Mn(1)-N(1)	89.3 (3)
O(1)#3-Mn(1)-O(3)	95.6 (3)	O(3)-Mn(1)-N(1)	72.1 (3)
O(2)-Mn(1)-O(4)#2	86.7 (3)	O(4)#2-Mn(1)-N(1)	117.7 (3)
O(1)#3-Mn(1)-O(4)#2	86.3 (4)	N(2)#1-Mn(1)-N(1)	81.8 (3)
O(3)-Mn(1)-O(4)#2	170.1 (3)	O(1)#3-Mn(1)-N(2)#1	167.0 (3)
O(2)-Mn(1)-N(2)#1	86.9 (4)	O(3)-Mn(1)-N(2)#1	90.6 (3)
O(4)#2-Mn(1)-N(2)#1	89.5 (3)		

Summetry code: #1 −x, y+1/2, −z+3/2; #2 x−1/2, −y+1/2, −z+1; #3 −x, y−1/2, −z+1/2.

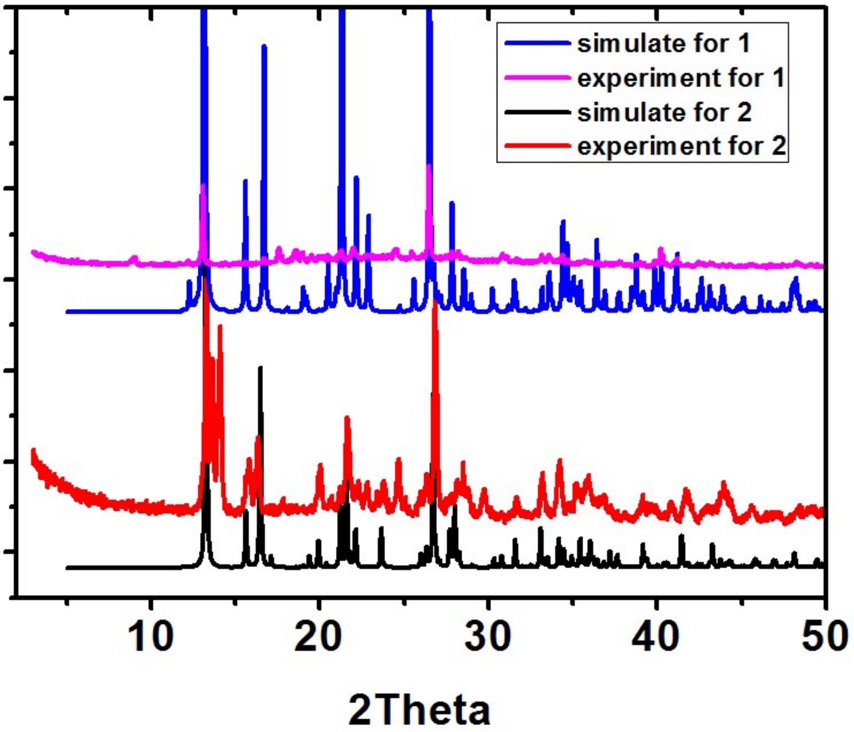

Figure S1. Simulated and experimental XRPD patterns for complexes **1** and **2**.

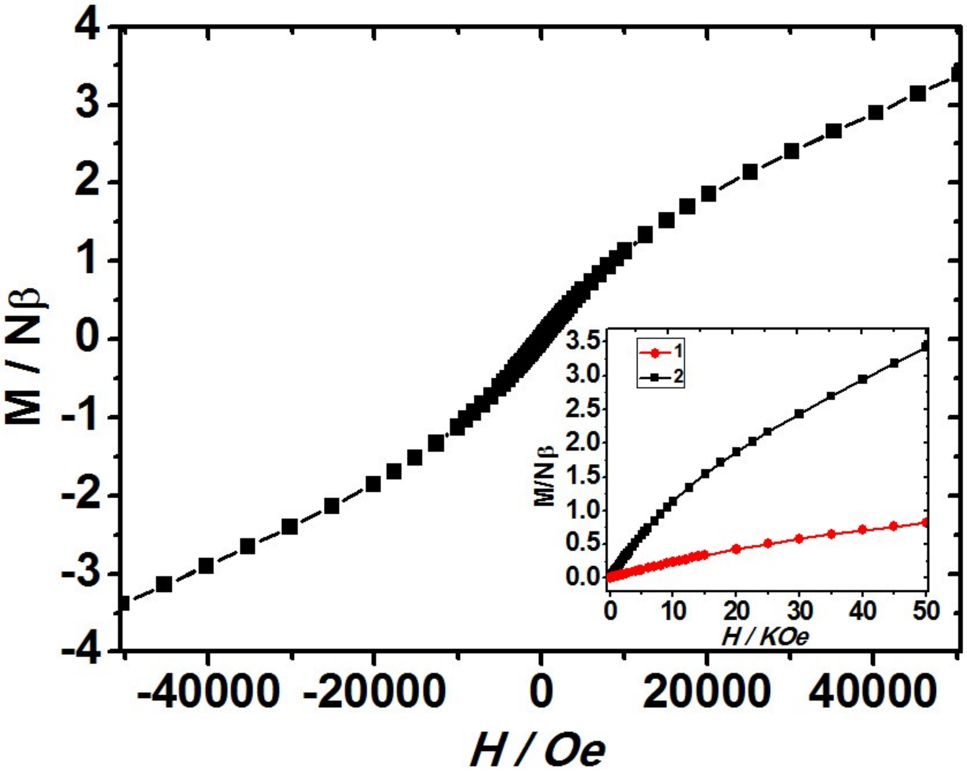

Figure S2. Hysteresis loop for **2**; insert: plot of the reduced magnetization for **1** and **2** at 2 K

Computational details

Calculation of Zero-Field Splitting Parameters *D* and *E* using NEVPT2

Complexes **1-2** (see Figure S3 for the calculated model structures of complexes **1** and **2**) are based on X-ray determined geometry.

To deeply analyse the magnetic anisotropy of complexes **1**and **2**, Orca 4.0 calculations[S3] were performed with N-Electron Valence State Perturbation Theory (NEVPT2)[S4] method. The spin-orbit coupling (SOC) operator used was the efficient implementation of the multicentre spin-orbit mean-field (SOMF) concept developed by Hess et al.[S5] The spin-spin contributions (SSC) to the *D* values were also included although they are very small for our complexes. All calculations were performed with triple-ζ with one polarization function TZVP[S6-S7] basis set for all atoms. Tight convergence criteria were used in order to ensure that the results are well converged with respect to technical parameters. The effective Hamiltonian implemented in Orca was used to extract the ZFS parameters *D* and *E*. Firstly, we carried out CASSCF calculation. And then, the effect of the dynamical electronic correlation was applied using NEVPT2 (Table S3). Our previous calculations[S8] show that NEVPT2 performed well on the calculations of zero-field splitting (ZFS) parameters *D* and *E* for transition metal-based magnets.

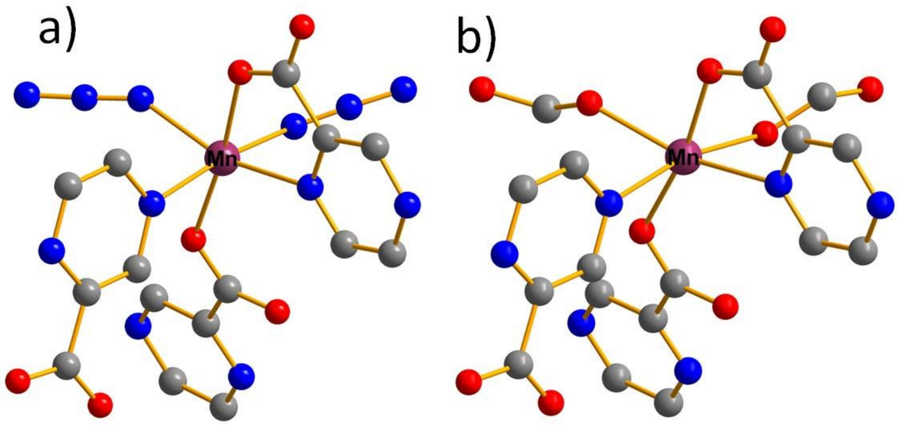

Figure S3. Calculated model structures of complexes **1** (a) and **2** (b). H atoms are omitted for clarity.

Table S3. Calculated zero-field splitting parameters D (E), single-ion $\mathrm{Mn^{II}}$ energy barrier Δ_A (cm^{-1}) and $\boldsymbol{g}$ (g_x, g_y, g_z) tensors of the lowest spin-orbit states of complexes **1** and **2** using NEVPT2.

	1	**2**
*S*pin	5/2	5/2
D(E)	0.04 (0.01)	−0.15 (−0.01)
Δ_A	0.0	0.9
	2.000	2.000
$\boldsymbol{g}$	2.000	2.000
	2.000	2.000

Estimation of the Exchange Interactions by B3LYP Calculations

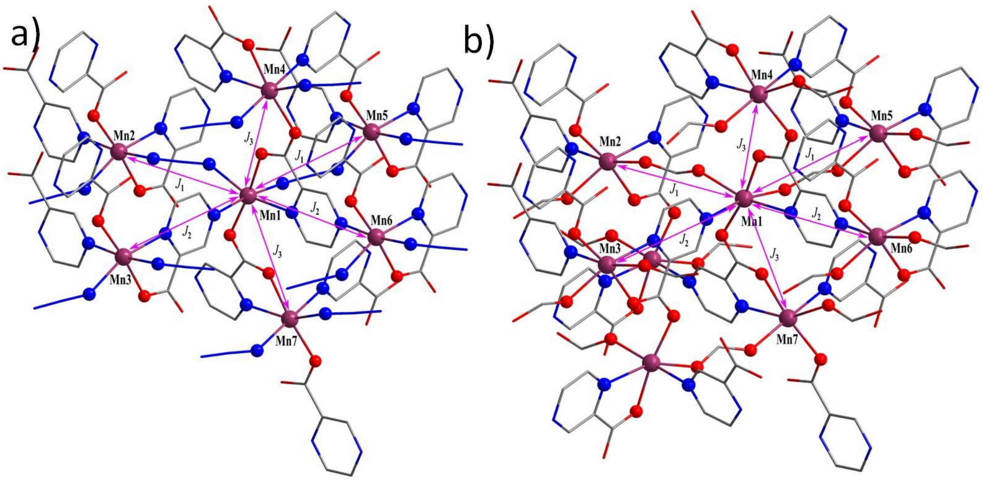

Figure S4. Structures of the labeled exchange coupling constants for complexes **1** (a) and **2** (b); H atoms are omitted.

To obtain the isotropic exchange coupling constants *J*, Orca 4.0 calculations[S3] were performed with the popular hybrid functional B3LYP proposed by Becke[S9-S10] and Lee et al.[S11] Triple-ζ with one polarization function TZVP [S6-S7] basis sets were used for all atoms, and zero order regular approximation (ZORA) was used for the scalar relativistic effect in all calculations. We have calculated three types of the $\mathrm{Mn^{II}}$-$\mathrm{Mn^{II}}$ exchange couplings. The corresponding exchange Hamiltonian is $\hat{H} = -2J_{\alpha}(\hat{S}_{\mathrm{Mn}_1}\hat{S}_{\mathrm{Mn}_i} + \hat{S}_{\mathrm{Mn}_1}\hat{S}_{\mathrm{Mn}_{i+3}})$ ($i = \alpha + 1$ while $\alpha = 1$, 2 and 3, respectively). The large integration grid (grid = 5) was applied to $\mathrm{Mn^{II}}$ for ZORA calculations. Tight convergence criteria were selected to ensure the results to be well converged with respect to technical parameters. Through calculating the energies of two spin states: the high-spin state ($S_{\mathrm{HS}} = S_{\mathrm{Mn1}} + S_{\mathrm{Mn}i} + S_{\mathrm{Mn}i+3}$, i = 2, 3 and 4), the broken-symmetry (BS) state (flip the spin on Mn1; $S_{\mathrm{BS}} = -S_{\mathrm{Mn1}} + S_{\mathrm{Mn}i} + S_{\mathrm{Mn}i+3}$, $i = 2$, 3 and 4), the isotropic $\mathrm{Mn^{II}}$-$\mathrm{Mn^{II}}$ coupling constants J_α (α = 1, 2 and 3) (Figure S4) were obtained by the Kahn's formula[S12]:

$$J = \frac{E_{BS} - E_{HS}}{60} \tag{1}$$

Table S4. Calculated J and the correlation energy barrier Δ_ξ ($\mathrm{cm^{-1}}$) values for complexes **1**–**2** using B3LYP.

	1	**2**
$J_1(\Delta_{\xi 1})$	−4.10 (102.5)	−0.61 (1.3)
$J_2(\Delta_{\xi 2})$	−0.02 (0.5)	−0.01 (0.0)
$J_3(\Delta_{\xi 3})$	−0.37 (9.3)	−0.85 (1.9)

In Table S4, the correlation energy barrier $\Delta_{\xi i} = 4J_iS_jS_k\cos\theta$ where θ is the included angle between the g_z directions on neighbouring Mn_j and Mn_k. For complex **1**, θ were all considered as zero since the very small D value of single-ion $\mathrm{Mn^{II}}$ is positive. For complex **2**, all of the included angles θ are close to 85°.

Reference

S1 *SAINT Software Mannual,* Bruker AXS :Madison, WI, 1998.

S2 G. M. Sheldrick, *SHELXTL NT*, version 5.1, University of GÖttingen: GÖttingen, Germany 1997.

S3 F. Neese, ORCA–*an ab initio, density functional and semiempirical program package*, version 4.0; Max-Planck institute for bioinorganic chemistry: Mülheim an der Ruhr, Germany, 2018.

S4 J. Miralles, O. Castell, R. Caballol and J. P. Malrieu, *Chem. Phys*., 1993, **172**, 33.

S5 B. A. Hess, C. M. Marian, U. Wahlgren and O. Gropen, *Chem. Phys. Lett.,* 1996, **251**, 365.

S6 A. Schafer, H. Horn and R. Ahlrichs, *J. Chem. Phys*., 1992, **97**, 2571.

S7 A. Schafer, C. Huber and R. Ahlrichs, *J. Chem. Phys.,* 1994, **100**, 5829.

S8 L. Chen, J. Wang, Y. Z. Liu, Y. Song, X. T. Chen, Y. Q. Zhang and Z. L. Xue, *Eur. J. Inorg. Chem*. 2015, 271-278.

S9 A. D. Becke, *J. Chem. Phys*., 1993, **98**, 5648.

S10 A. D. Becke, *Phys. Rev. A.,* 1988, **38**, 3098.

S11 C. Lee, W. Yang and R. G. Parr, *Phys. Rev. B*., 1988, **37**, 785.

S12 K. Olivier, *Molecular Magnetism*, 1993, 211.